

# Critical exponents in coupled phase-oscillator models on small-world networks

Ryosuke Yoneda, Kenji Harada, and Yoshiyuki Y. Yamaguchi  
*Graduate School of Informatics, Kyoto University, 606-8501 Kyoto, Japan*

A coupled phase-oscillator model consists of phase-oscillators, each of which has the natural frequency obeying a probability distribution and couples with other oscillators through a given periodic coupling function. This type of models is widely studied since it describes the synchronization transition, which emerges between the non-synchronized state and partially synchronized states, and which is characterized by the critical exponents. Among them, we focus on the critical exponent defined by coupling strength dependence of the order parameter. The synchronization transition is not limited in the all-to-all interaction, whose number of links is of  $O(N^2)$  with  $N$  oscillators, and occurs in small-world networks whose links are of  $O(N)$ . In the all-to-all interaction, values of the critical exponent depend on the natural frequency distribution and the coupling function, classified into an infinite number of universality classes. A natural question is in small-world networks, whether the dependency remains irrespective of the order of links. To answer this question we numerically compute the critical exponent on small-world networks by using the finite-size scaling method with coupling functions up to the second harmonics and with unimodal and symmetric natural frequency distributions. Our numerical results suggest that, for the continuous transition, the considered models share the critical exponent  $1/2$ , and that they are collapsed into one universality class.

## I. INTRODUCTION

Ever since Huygens found that two pendulum clocks hanging on a wall swung in the opposite direction from each other, many illustrations of synchronization have been established in various fields of nature, such as frog choruses [1], flashing of fireflies [2, 3], metronomes [4], and circadian rhythms [5]. It is natural to try to understand synchronization theoretically, and a coupled phase-oscillator model is one of successful models to describe synchronization [6]. This model consists of many coupled oscillators, and the coupling is expressed by a periodic coupling function. Each oscillator has the so-called natural frequency, randomly drawn from a natural frequency distribution. When the coupling strength  $K$  increases, the oscillators exhibit the synchronization transition from the non-synchronized state to (partially) synchronized states. The synchronization transition is continuous or discontinuous, depending on the natural frequency distribution and the coupling function [7–17].

The critical phenomena have been extensively studied in statistical mechanics. One of their remarkable features is the existence of universality classes; the systems in a universality class share the critical exponents defined around the critical point  $K_c$  of a continuous transition. One of the critical exponents is  $\beta$ , defined by  $r \sim (K - K_c)^\beta$ , where  $r$  is the order parameter. Thus, it is natural to ask the universality classes in the coupled phase-oscillator models through values of the critical exponent  $\beta$ .

For the all-to-all and uniform coupling, extended researches have computed the value of  $\beta$ , and it depends on the coupling function and the natural frequency distribution [7–17]. For simplicity, we focus on coupling functions which have two harmonics at most, and review values of the critical exponent  $\beta$  for the following three cases: (i) the second harmonics is absent, (ii) the second

harmonics has the opposite sign with the leading harmonics, and (iii) the second harmonics has the same sign with the leading harmonics. We assume that the natural frequency distribution is unimodal and symmetric, and that the second-leading term of its Maclaurin expansion is of the order  $2n$ .

In the case (i) and (ii), the model shows a continuous transition, whereas in the case (iii), a discontinuous transition occurs, hence we cannot define the critical exponent  $\beta$  [12]. In the case (i), the model becomes the Kuramoto model [7], a paradigmatic coupled phase-oscillator model. Several researches have pointed out that the critical exponent  $\beta = 1/(2n)$  [7–10]. This  $n$  dependence is a strong feature of the Kuramoto model and gives a sharp contrast with the case (ii). In the case (ii), the critical exponent  $\beta$  becomes 1 for  $n = 1$  [11–14], and this value is suggested to be universal irrespective of  $n \in \mathbb{N}$  [12].

The universality of the coupled phase-oscillator models depends also on the manner of coupling, that is, the network of the coupling. For example, oscillator models on complex networks are of interest to many natural phenomena [18]. In particular, a previous research [19] has studied the continuous synchronous transition of the coupled phase-oscillator model on a small-world network, one of complex networks, and claims that  $\beta = 1/2$  for  $n = 1$  in the case (i). However, the research lacks to consider other cases. In this paper, we numerically study the synchronous transitions on small-world networks in the cases (i)-(iii) above. Our results suggest that in the case (i) and (ii), a continuous transition occurs, and  $\beta = 1/2$  for every  $n \in \mathbb{N}$ .

This paper is organized as follows. In Sec. II, we show the algorithm of constructing the small-world network, then introduce coupled phase-oscillator models on small-world networks. We also introduce a family of the natural frequency distributions, whose second-leading term is of

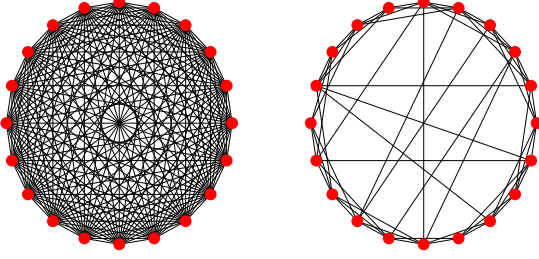


FIG. 1. Comparison between the all-to-all network (left) and a small-world network (right) with 20 nodes. In the small-world network, we set  $k = 3$  and the rewiring probability  $p = 0.2$ .

the order  $2n$ . In Sec. III, we show a way to calculate the critical exponent  $\beta$  using finite-size scaling, then we numerically obtain  $\beta$ . Finally, in Sec. IV, we summarize this paper and note some future works.

## II. COUPLED PHASE-OSCILLATOR MODELS ON SMALL-WORLD NETWORKS

In this section, we define the coupled phase-oscillator model on a small-world network, and introduce the order parameter to observe synchronization. A small-world network possesses the property of a small diameter and a large clustering coefficient despite its sparsity. This network can be seen in various fields of the real world, such as human relationships, World Wide Web, citations of scientific papers, and so on. In 1998, Watts and Strogatz proposed a breakthrough network model showing the property of a small-world network, which is created in the following algorithm [20]. We first make a periodic  $k$ -nearest neighbor network with  $N$  nodes, which results in  $kN$  edges. Then we rewire each edge with probability  $p$ , keeping in mind that we do not allow self-loops or link duplications. Also, we use only connected small-world networks: if a generated network is disconnected, we discard it and generate another one until connected one is created. See Fig. 1 for a comparison between the all-to-all network and a small-world network. In this paper, we set  $k = 3$  and  $p = 0.2$ , following the previous research on the coupled phase-oscillator model on a small-world network [19].

We consider the coupled phase-oscillator model with  $N$  oscillators on a small-world network, which evolves in time with the following equations,

$$\begin{aligned} \frac{d\theta_i}{dt} &= \omega_i + \frac{K}{2k} \sum_{j \in \Lambda_i} f_a(\theta_j - \theta_i), \\ f_a(\theta) &= \sin \theta + a \sin 2\theta, \end{aligned} \quad (1)$$

for  $i = 1, \dots, N$ .  $\theta_i$  and  $\omega_i$  are the phase and the natural frequency of the  $i$ th oscillator respectively, and  $\omega_i$  is ran-

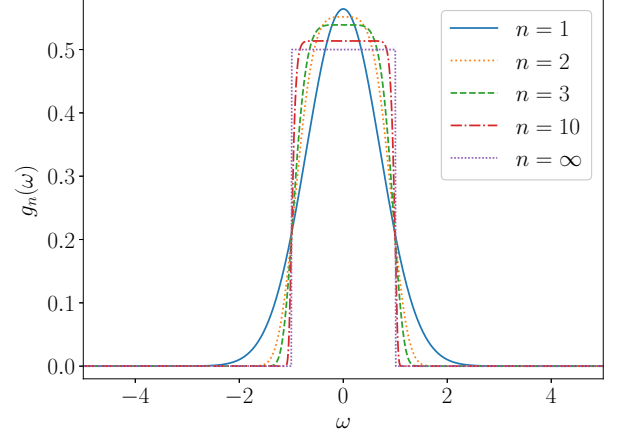


FIG. 2. Graphs of  $g_n(\omega)$  with  $n = 1, 2, 3, 10$ , and  $\infty$ , where we set  $\Delta = 1$ . We see that the  $g_n(\omega)$  converges to  $g_\infty(\omega)$  as  $n$  becomes larger.

domly drawn from a natural frequency distribution  $g(\omega)$ .  $K > 0$  is a coupling constant, describing how strong the coupling between oscillators are.  $\Lambda_i$  is the index set, which contains the indexes of oscillators connecting to the  $i$ th oscillator. For each oscillator, the average number of edges is  $2k$ , and we normalize the coupling term by  $2k$ . The coupling function is  $f_a(\theta)$ , and when  $a = 0$ , this model is identical to the one proposed in [19].

As the natural frequency distribution  $g(\omega)$ , we introduce a family of distributions, parametrized by a natural number  $n \in \mathbb{N}$ ,

$$g_n(\omega) = \frac{n}{\Gamma(1/(2n))\Delta} e^{-(\omega/\Delta)^{2n}}, \quad (2)$$

where  $\Gamma(z) = \int_0^\infty t^{z-1} e^{-t} dt$  is the Gamma function defined on  $\Re(z) > 0$ . Here,  $\Delta > 0$  is a parameter describing the width of the distribution. We note that  $n = 1$  gives the Gaussian distribution. For every  $n$ , this distribution is unimodal and symmetric with respect to  $\omega = 0$ , and its Maclaurin expansion has the following form,

$$g_n(\omega) = g_n(0) - C_n \omega^{2n} + \dots, \quad (3)$$

where  $C_n = n/(\Gamma(1/(2n))\Delta^{2n+1})$  is positive. We remark that the generalized Lorentzian distribution introduced in [21] also has the same expansion form. In the limit  $n \rightarrow \infty$ ,  $g_n(\omega)$  converges to  $g_\infty(\omega)$  in the  $L^1$ -norm,

$$g_\infty(\omega) = \begin{cases} 1/(2\Delta), & \omega \in (-\Delta, \Delta), \\ 0, & \text{otherwise.} \end{cases} \quad (4)$$

This distribution is a uniform distribution on a compact support. See Fig. 2 for the graph of the distribution  $g_n(\omega)$  and its convergence to  $g_\infty(\omega)$ .

To visualize the extent of synchronization of oscillators, we introduce the order parameter  $r_N(K)$  defined for each

coupling strength  $K$ ,

$$r_N(K) = \left| \frac{1}{N} \sum_{j=1}^N e^{i\theta_j} \right|. \quad (5)$$

This order parameter represents the centroid of the oscillators moving on the complex unit circle  $\mathbb{S}^1$ . When the oscillators are uniformly distributed on  $\mathbb{S}^1$ , which corresponds to the non-synchronized state,  $r_N(K)$  gets close to 0. On the other hand, when the oscillators gather at a point on  $\mathbb{S}^1$ , which corresponds to the synchronized state,  $r_N(K)$  equals 1. Calculating  $r_N(K)$  is therefore useful for monitoring synchronization of the coupled phase-oscillator models. In the next section, we will look into the relationship between the order parameter  $r_N(K)$  and the coupling strength  $K$ .

We remark a difference between the model considered in [22, 23] and ours. In the literature, the authors consider the coupled phase-oscillator models on the small-world network with the equivalent equations as (1), but they construct the small-world network with each node connected to  $k = \lfloor sN \rfloor$  neighbors for  $s \in (0, 0.5)$ , whereas  $k$  is constant regardless of  $N$  in our model. Here,  $\lfloor x \rfloor$  is the floor function that takes the greatest integer less than or equal to  $x$ . As a result, their network has  $O(N^2)$  edges, and is much more dense than our network, which has  $O(N)$  edges. An advantage of their model is that it can be analyzed through the equation of continuity using the graphon [24], the continuous limit of the matrix representing the couplings, of the small-world network.

We note the dependency on  $p$  for a synchronization transition. For  $p = 0$ , the small-world network becomes the periodic one-dimensional  $k$ -nearest-neighbor network. In [19], the authors numerically showed that a coupled phase-oscillator model on a  $k$ -nearest-neighbor network does not show a synchronization transition;  $r \approx 0$  for all  $K$ . However, if  $p$  is greater than zero, a synchronization transition occurs because of emergence of shortcuts.

### III. NUMERICAL SIMULATIONS

In the large population limit  $N \rightarrow \infty$ , the coupled phase-oscillator model (1) is expected to show a synchronization transition around a critical point  $K_c$ . For  $K < K_c$ , the order parameter  $r(K) := \lim_{N \rightarrow \infty} r_N(K)$  is zero, which corresponds to the non-synchronized state. On the other hand, for  $K > K_c$ , the model shows a partial synchronized state, in which  $r(K)$  exhibits power law behavior close to the critical point in the form of

$$r(K) \sim (K - K_c)^\beta, \quad (6)$$

where  $\beta$  is one of the critical exponents. The critical exponents are crucial to describe critical phenomena, and models are classified into universality classes, each of which shares the same critical exponents. Therefore

calculating the critical exponents, including  $\beta$ , is an important problem from theoretical and numerical perspectives. In this section, we numerically calculate the critical exponent  $\beta$  of the coupled phase-oscillator models on small-world networks.

The critical exponent  $\beta$  is defined in the large population limit  $N \rightarrow \infty$ , and this cannot be achieved through the numerical simulations. To overcome this difficulty, we use the finite-size scaling, that is, we assume that there exists a function  $F$ , so called the scaling function, and that the order parameter reads

$$r_N(K) = N^{-\beta/\bar{\nu}} F((K - K_c)N^{1/\bar{\nu}}). \quad (7)$$

Here, the critical exponent  $\bar{\nu}$  is defined through the correlation length  $\xi$ , which diverges at  $K = K_c$  with

$$\xi \propto (K - K_c)^{-\bar{\nu}}. \quad (8)$$

The finite-size scaling is widely used for numerical studies of critical phenomena in second-order phase transitions, including coupled phase-oscillator models [19, 25–30]. In this paper, we use a new statistical method [31, 32] to estimate the values of  $K_c$ ,  $\beta$  and  $\bar{\nu}$  in the finite-size scaling relation. Using a new technique in the field of machine learning, we can automatically find the best parameter set with a good collapse of data points onto a scaling function  $F$ .

Numerical simulations of the coupled phase-oscillator model on the small-world networks are performed by using the fourth-order Runge–Kutta algorithm with the time step  $\delta t = 0.1$ . We first make a Watts–Strogatz’s small-world network, and for each  $K$ , we numerically integrate (1) by setting random initial phases and random natural frequencies obeying  $g_n(\omega)$ , and we take the time average of the order parameter in the time interval  $t \in [300, 500]$ . We performed 400 realizations by changing small-world networks for each system size, which we take from  $N = 1600$  to  $N = 25600$ . The order parameter  $r_N(K)$  and its errorbar are evaluated by the resampling technique: We randomly choose 200 samples out of 400 realizations, and we calculate the mean of the order parameter, which we refer to  $\{r_N^{(i)}(K)\}_{i=1}^S$ . We take this step for  $S = 1000$  times, and  $r_N(K)$  is given by the mean of  $\{r_N^{(i)}(K)\}_{i=1}^S$ , and the confidence interval of  $r_N(K)$  is given by the statistical deviation of  $\{r_N^{(i)}(K)\}_{i=1}^S$ . We will show results of  $a = 0, -0.2$ , and  $0.5$ , chosen from the neighborhood of  $a = 0$ , as the case (i), (ii), and (iii), respectively. The order of the second-leading term in the natural frequency distribution are taken as  $n = 1, 2, 3$ , and  $\infty$ . See Fig. 3 for the numerical results with  $n = 1$  and  $a = 0, -0.2$ .

Once we obtain  $r_N(K)$  for several system size  $N$ , we evaluate the critical exponents  $\beta$  and  $\bar{\nu}$  and the critical point  $K_c$  from the scaling relation (7). We determine these values by finding the best values so that points of  $r_N(K)N^{\beta/\bar{\nu}}$  as a function of  $(K - K_c)N^{1/\bar{\nu}}$  are tightly collapsed to a scaling function  $F$ . Here we again use the resampling method to obtain the critical exponents

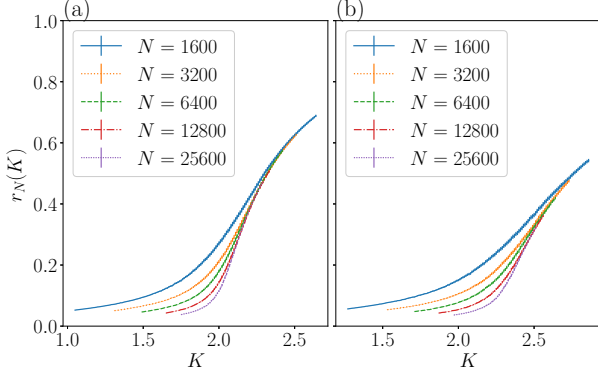


FIG. 3. Graphs of order parameter  $r_N(K)$  with its confidence interval for the model (1), where we take the coupling function  $f_a(\theta)$  with (a)  $a = 0$  and (b)  $a = -0.2$ . As a natural frequency distribution, we use  $g_1(\omega)$  with  $\Delta = 1$ , and  $N = 1600, 3200, 6400, 12800$ , and  $25600$  from top to bottom.  $r_N(K)$  and its confidence interval are evaluated by the resampling technique. Errorbars are so small that they may not be visible.

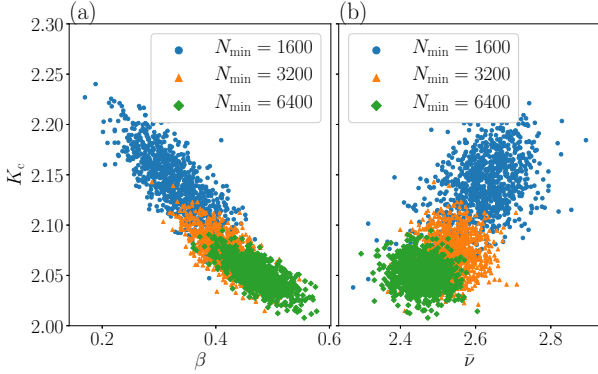


FIG. 4. Scattering plots of computed parameters  $K_c, \beta$  and  $\bar{\nu}$ , evaluated by the Bayesian scaling analysis. Here, we use  $(a, n) = (0, 1)$ , and we set  $N_{\min}$  to 1600, 3200 and 6400.

and their confidence intervals: By introducing the symbol  $N_{\min}$  to indicate the smallest system size for the finite-size scaling analysis, we use  $r_{N_{\min}}^{(i)}(K), r_{2 \cdot N_{\min}}^{(i)}(K)$ , and  $r_{4 \cdot N_{\min}}^{(i)}(K)$  to evaluate  $\beta, \bar{\nu}$ , and  $K_c$  by the Bayesian scaling analysis [31, 32]. Figure 4 shows  $\beta, \bar{\nu}$ , and  $K_c$  estimated from each resampling data set. Mean values and standard deviations of  $\beta, \bar{\nu}$ , and  $K_c$  give us the best-fit parameters and confidence intervals. We carried out this procedure for  $N_{\min} = 1600, 3200$ , and  $6400$ . The graph of  $r_N(K)N^{\beta/\bar{\nu}}$  versus  $(K - K_c)N^{1/\bar{\nu}}$  are shown in Fig. 5 for checking the validity of the estimated parameters  $\beta, \bar{\nu}$ , and  $K_c$ .

We check the hysteresis of (1) with  $a = 0.5$  by taking two different types of initial phases  $\{\theta_i\}_{i=1}^N$ : (i) We start with the random initial phases  $\{\theta_i\}_{i=1}^N$  at  $K = K_{\text{start}}$ , and the final phases at  $t = 500$  is used as the initial

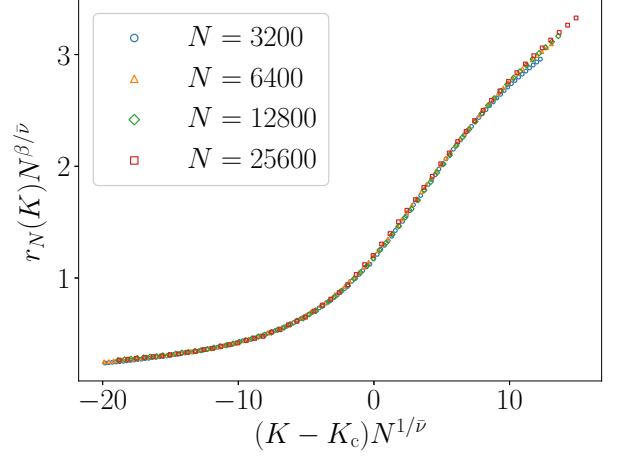


FIG. 5. Graph of scaled order parameter  $r_N(K)N^{\beta/\bar{\nu}}$  versus scaled coupling constant  $(K - K_c)N^{1/\bar{\nu}}$  for  $(a, n) = (0, 1)$ , where we use  $\beta, \bar{\nu}$  and  $K_c$ , obtained by the Bayesian scaling analysis for  $N_{\min} = 6400$ . The values of  $\beta, \bar{\nu}$ , and  $K_c$  are shown in Table I. We see that the scaled data are well collapsed to a scaling function  $F$ .

phases at the successive value of  $K$  in the increasing direction. We call this process the “forward” process, and  $r_N^{(\text{forward})}(K)$  denotes its order parameter. (ii) Contrary to the “forward” process, we start with the random initial phases  $\{\theta_i\}_{i=1}^N$  at  $K = K_{\text{end}}$ , and the final phases at  $t = 500$  is used as the initial phases at the successive value of  $K$  in the decreasing direction. We call this process the “backward” process, and  $r_N^{(\text{backward})}(K)$  denotes its order parameter. We have executed the numerical simulations of (1) for  $a = 0, -0.2$ , and  $0.5$ , and  $n = 1, 2, 3$ , and  $\infty$ , and  $N = 25600$  with two different initial phases as shown above, and confirmed that there exists a hysteresis only for  $a = 0.5$  regardless of  $n$ . See Fig. 6 for an example of a hysteresis with  $(a, n) = (0.5, 1)$ . We therefore conclude that the coupled phase-oscillator model (1) shows a discontinuous transition for  $a = 0.5$ .

Results of the parameters estimated by the Bayesian scaling analysis are summarized in Table I. Here we extrapolate the critical values to  $N_{\min} = \infty$  by plotting the values of  $K_c, \beta$  and  $\bar{\nu}$  as a function of  $1/N_{\min}$ , and use the least square method to find the values at  $\lim_{N_{\min} \rightarrow \infty} 1/N_{\min} = 0$ . The extrapolated values are listed in the line of  $N_{\min} = \infty$  in Table I. See Fig. 7 for the extrapolation of  $\beta$  with  $a = 0$  and  $-0.2$ .

By observing the computed parameters shown in Table I, we find that  $\beta$  converge to

$$\beta \simeq \frac{1}{2}, \quad (9)$$

which is independent of  $a$  and  $n$ , unlike the coupled phase-oscillator on the all-to-all network. We notice that the critical exponent  $\bar{\nu}$  obtained in [19], claiming that  $\bar{\nu} \simeq 2$  for  $(a, n) = (0, 1)$ , is different from ours,

TABLE I. Critical exponents  $\beta, \bar{\nu}$  and the critical point  $K_c$  of (1) depending on the coupling function  $f_a(\theta) = \sin \theta + a \sin 2\theta$  and the natural frequency distribution  $g_n(\omega)$  in (2), for  $a = 0$  and  $-0.2$  and  $n = 1, 2, 3$ , and  $\infty$ . For each pair of  $(a, n)$ , we use  $N_{\min} = 1600, 3200, 6400$ , and execute the Bayesian scaling analysis [31] to find the best parameters fitting (7). We extrapolate the critical values to  $N_{\min} = \infty$  by using the least square method, and they are listed in the line of  $N_{\min} = \infty$ .

$f_a(\theta)$	$g_n(\omega)$	$N_{\min}$	$K_c$	$\beta$	$\bar{\nu}$
$a = 0$	$n = 1$	1600	2.13(3)	0.33(4)	2.61(7)
		3200	2.07(1)	0.42(3)	2.53(5)
		6400	2.05(1)	0.47(3)	2.45(4)
		$\infty$	<b>2.02(2)</b>	<b>0.51(4)</b>	<b>2.40(6)</b>
	$n = 2$	1600	1.85(1)	0.27(2)	2.67(5)
		3200	1.78(1)	0.37(2)	2.53(3)
		6400	1.755(9)	0.44(2)	2.50(3)
		$\infty$	<b>1.72(1)</b>	<b>0.49(2)</b>	<b>2.43(4)</b>
	$n = 3$	1600	1.80(1)	0.28(2)	2.62(4)
		3200	1.76(1)	0.33(2)	2.51(3)
		6400	1.723(8)	0.44(2)	2.51(3)
		$\infty$	<b>1.69(1)</b>	<b>0.47(2)</b>	<b>2.46(4)</b>
	$n = \infty$	1600	1.83(1)	0.27(1)	2.50(4)
		3200	1.79(1)	0.36(2)	2.52(3)
		6400	1.780(8)	0.41(2)	2.46(3)
		$\infty$	<b>1.76(1)</b>	<b>0.46(2)</b>	<b>2.46(4)</b>
$a = -0.2$	$n = 1$	1600	2.43(5)	0.38(8)	2.67(9)
		3200	2.35(2)	0.44(6)	2.58(7)
		6400	2.34(1)	0.45(4)	2.42(6)
		$\infty$	<b>2.31(3)</b>	<b>0.48(6)</b>	<b>2.36(8)</b>
	$n = 2$	1600	2.09(3)	0.31(4)	2.87(7)
		3200	1.99(2)	0.41(4)	2.65(5)
		6400	1.96(1)	0.47(3)	2.52(4)
		$\infty$	<b>1.91(2)</b>	<b>0.51(4)</b>	<b>2.41(6)</b>
	$n = 3$	1600	2.04(3)	0.27(5)	2.85(8)
		3200	1.96(2)	0.37(4)	2.65(5)
		6400	1.91(1)	0.49(3)	2.59(4)
		$\infty$	<b>1.86(2)</b>	<b>0.55(4)</b>	<b>2.50(6)</b>
	$n = \infty$	1600	2.08(3)	0.25(4)	2.76(6)
		3200	2.00(1)	0.38(4)	2.69(5)
		6400	1.97(1)	0.43(3)	2.54(4)
		$\infty$	<b>1.94(2)</b>	<b>0.49(4)</b>	<b>2.49(6)</b>

$\bar{\nu} \simeq 5/2$ . They first find the best fit  $\beta/\bar{\nu}$  and  $K_c$  at which  $r_N(K)N^{\beta/\bar{\nu}}$  crosses at  $K = K_c$  by varying the system size  $N$ . Then they use the following formula,

$$\log \left[ \frac{dr_N}{dK}(K_c) \right] = \frac{1-\beta}{\bar{\nu}} \log N + \text{const.}, \quad (10)$$

which is calculated by taking the derivative of (7) with respect to  $K$ , and they calculate  $(1-\beta)/\bar{\nu}$  by computing the slope of  $\log[\frac{dr_N}{dK}(K_c)]$  with respect to  $\log N$ . However this method has a disadvantage that the estimated critical point  $K_c$  is needed for calculating  $(1-\beta)/\bar{\nu}$ . Also, this method does not take into account the numerical results  $r_N(K)$  for  $K \neq K_c$ . We believe that our estimation of the critical exponents is more reliable because it uses the Bayesian scaling analysis which overcomes these disadvantages.

#### IV. CONCLUSION AND DISCUSSION

We calculated the critical exponents  $\beta$  and  $\bar{\nu}$  for the coupled phase-oscillator models on the small-world network in (1) by using the finite-size scaling method. We set the coupling function as  $f_a(\theta) = \sin \theta + a \sin 2\theta$ , and the natural frequency distribution as  $g_n(\omega)$  in (2), and we studied the  $(a, n)$ -dependency of the critical exponent  $\beta$ . Our results suggest that  $\beta$  is  $1/2$  for all  $g_n(\omega)$  and coupling function  $f_a(\theta)$  with  $a = 0$  and  $-0.2$ , which means that all such systems are in the same universality class. This universality shows a sharp contrast with the Kuramoto model, which has various values of  $\beta$  depending on the coupling function and the natural frequency distribution. Remarking that the coupled phase-oscillator models on a small-world network with  $O(N^2)$  edges [22, 23] shares the same critical exponent as the Kuramoto model, whose network also has  $O(N^2)$  edges, we believe that this contrast comes from the number of edges of networks. We also find that the model (1) shows

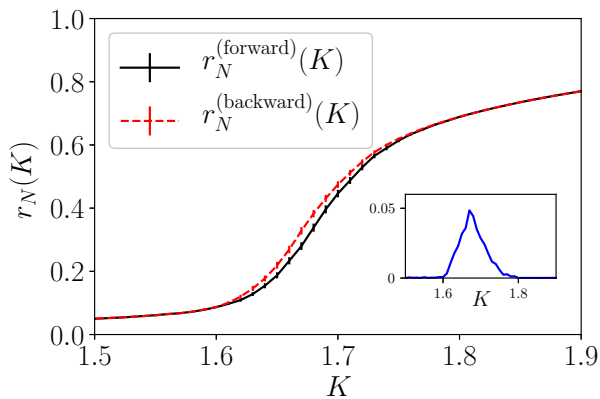


FIG. 6. Graphs of  $r_N(K)$  and its errorbar of (1) for  $(a, n) = (0.5, 1)$  with two different types of initial phases, where we set the number of oscillators  $N = 25600$ . We see that  $r_N(K)$  takes a different value depending on the choice of the initial phases around  $K \in (1.6, 1.8)$ . The inset shows that the graph of  $r_N^{(\text{backward})}(K) - r_N^{(\text{forward})}(K)$ .

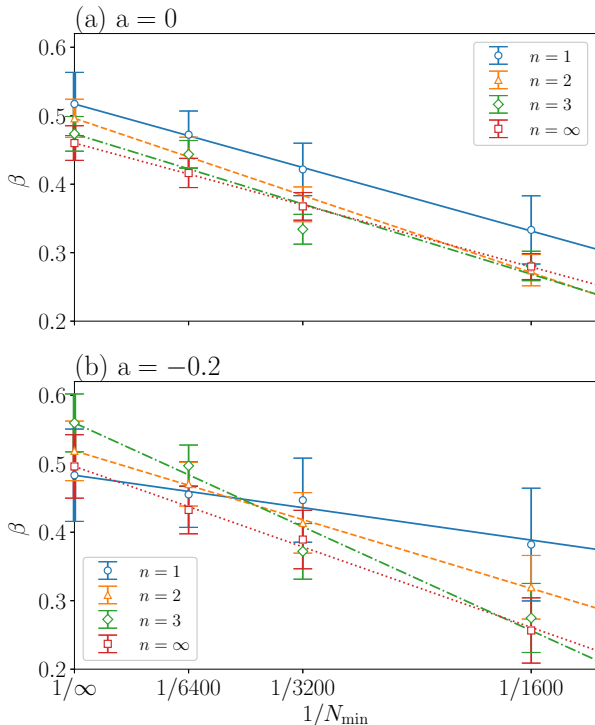


FIG. 7. Graphs of  $\beta$  as a function of  $1/N_{\min}$  for (a)  $a = 0$  and (b)  $a = -0.2$  in (1). Critical exponents obtained by the finite-size scaling are shown with errorbars, and their extrapolation are shown at  $1/N_{\min} = 1/\infty$ , which are calculated by the least square method. For each  $a$ , the resulting linear regression lines are drawn with the solid line for  $n = 1$ , the dashed line for  $n = 2$ , the dot-dashed line for  $n = 3$ , and the dotted line for  $n = \infty$ .

a discontinuous transition for  $a = 0.5$ . This discontinuity is shared between the two types of networks: networks with  $O(N^2)$  edges and  $O(N)$  edges.

We end this paper commenting on five future works. Firstly, we mainly focused on the dependence of critical exponents of the natural frequency distribution, and we picked representative points of  $a$  from around  $a = 0$  to check universality in the coupled phase-oscillator models on a small-world network. Studying a global phase diagram on the  $(K, a)$ -plane is a subject for future research.

Secondly, we note a relationship with the noisy Kuramoto model. In the Kuramoto model, the value of  $\beta$  depends on the natural frequency distribution, but by adding some noises,  $\beta = 1/2$  is consistent regardless of the natural frequency distribution [33]. This value is similar to the one in the coupled phase-oscillator models on a small-world network with a reasonable choice of the  $1/N$  extrapolation performed in Fig. 7. These coincidence thus suggests introducing the small-world network plays a similar role with applying noises because of its inhomogeneous couplings.

Thirdly, in addition to the critical exponent  $\beta$ , there are still other critical exponents to calculate,  $\gamma$  and  $\delta$  concerning with response for instance. Once we obtain three critical exponents, we can check if the Widom equality  $\gamma = \beta(\delta - 1)$  holds. For the Kuramoto model, the Widom equality is obtained by analyzing the self-consistent equation with respect to  $r$  [10]. However, we cannot derive the self-consistent equation for the coupled phase-oscillator model on the small-world network, and it is not obvious if the Widom equality holds.

Fourthly, it remains to clarify  $\alpha$ -dependence of the critical exponent  $\beta$  in coupled phase-oscillator models with  $O(N^\alpha)$ -edge networks ( $1 < \alpha < 2$ ). This  $\alpha$ -dependence may make a bridge to the gap between  $\alpha = 2$  and 1, which has been revealed in this paper.

Finally, since we numerically obtained  $\beta$ , it is natural to check the value theoretically. To investigate critical phenomena in the model (1), one has to consider the large population limit  $N \rightarrow \infty$ , but to the best of our knowledge, we do not have a tool for taking the large population limit with network of  $O(N)$  edges. It is challenging to attack this problem.

## ACKNOWLEDGMENTS

In this research work we used the supercomputer of ACCMS, Kyoto University. Y.Y.Y. acknowledges the support of JSPS KAKENHI Grant No. 16K05472.

- 
- [1] I. Aihara, T. Mizumoto, T. Otsuka, H. Awano, K. Nagira, H. G. Okuno, and K. Aihara, Spatio-Temporal Dynamics in Collective Frog Choruses Examined by Mathematical Modeling and Field Observations, *Sci. Rep.* **4**, 3891 (2014).
  - [2] H. M. Smith, Synchronous flashing of fireflies, *Science* **82**, 151 (1935).
  - [3] J. Buck and E. Buck, Mechanism of rhythmic synchronous flashing of fireflies, *Science* **159**, 1319 (1968).
  - [4] J. Pantaleone, Synchronization of metronomes, *Am. J. Phys.* **70**, 992 (2002).
  - [5] A. T. Winfree, Biological Rhythms and the Behavior of Populations of Coupled Oscillators, *J. Theoret. Biol.* **16**, 15 (1967).
  - [6] Y. Kuramoto and H. Nakao, On the concept of dynamical reduction: the case of coupled oscillators, *Phil. Trans. R. Soc. A* **377**, 20190041 (2019).
  - [7] Y. Kuramoto, Self-entertainment of a population of coupled non-linear oscillators, *International Symposium on Mathematical Problems in Theoretical Physics, Lecture Notes in Physics* **39**, 420 (1975).
  - [8] S. H. Strogatz, From Kuramoto to Crawford: exploring the onset of synchronization in populations of coupled oscillators, *Physica D* **143**, 1 (2000).
  - [9] H. Chiba, A proof of the Kuramoto conjecture for a bifurcation structure of the infinite-dimensional Kuramoto model, *Ergod. Th. & Dynam. Sys.* **35**, 762 (2015).
  - [10] H. Daido, Susceptibility of large populations of coupled oscillators, *Phys. Rev. E* **91**, 012925 (2015).
  - [11] J. D. Crawford, Scaling and Singularities in the Entrainment of Globally Coupled Oscillators, *Phys. Rev. Lett.* **74**, 4341 (1995).
  - [12] H. Chiba and I. Nishikawa, Center manifold reduction for large populations of globally coupled phase oscillators, *Chaos* **21**, 043103 (2011).
  - [13] M. Komarov and A. Pikovsky, Multiplicity of Singular Synchronous States in the Kuramoto Model of Coupled Oscillators, *Phys. Rev. Lett.* **111**, 204101 (2013).
  - [14] M. Komarov and A. Pikovsky, The Kuramoto model of coupled oscillators with a bi-harmonic coupling function, *Physica D* **289**, 18 (2014).
  - [15] L. Basnarkov and V. Urumov, Phase transitions in the Kuramoto model, *Phys. Rev. E* **76**, 057201 (2007).
  - [16] D. Pazó, Thermodynamic limit of the first-order phase transition in the Kuramoto model, *Phys. Rev. E* **72**, 046211 (2005).
  - [17] H. Daido, Intrinsic Fluctuations and a Phase Transition in a Class of Large Populations of Interacting Oscillators, *J. Stat. Phys.* **60**, 753 (1990).
  - [18] S. N. Dorogovtsev, A. V. Goltsev, and J. F. F. Mendes, Critical phenomena in complex networks, *Rev. Mod. Phys.* **80**, 1275 (2008).
  - [19] H. Hong, M. Y. Choi, and B. J. Kim, Synchronization on small-world networks, *Phys. Rev. E* **65**, 026139 (2002).
  - [20] D. J. Watts and S. H. Strogatz, Collective dynamics of ‘small-world’ networks, *Nature* **393**, 440 (1998).
  - [21] B. Pietras, N. Deschle, and A. Daffertshofer, First-order phase transitions in the Kuramoto model with compact bimodal frequency distributions, *Phys. Rev. E* **98**, 062219 (2018).
  - [22] H. Chiba, G. S. Medvedev, and M. S. Mizuhara, Bifurcations in the Kuramoto model on graphs, *Chaos* **28**, 073109 (2018).
  - [23] G. S. Medvedev, Small-world networks of Kuramoto oscillators, *Physica D* **266**, 13 (2014).
  - [24] L. Lovasz, Large networks and graph limits, (American Mathematical Society, Providence, Rhode Island, 2012).
  - [25] A. Pelisseto and E. Vicari, Critical phenomena and renormalization-group theory, *Phys. Rep.* **368**, 549 (2002).
  - [26] M. Hasenbusch, Finite size scaling study of lattice models in the three-dimensional Ising universality class, *Phys. Rev. B* **82**, 174433 (2010).
  - [27] A. Pikovsky and M. Rosenblum, Dynamics of globally coupled oscillators: Progress and perspectives, *Chaos* **25**, 097616 (2015).
  - [28] H. Hong, H. Chaté, L-H. Tang, and H. Park, Finite-size scaling, dynamic fluctuations, and hyperscaling relation in the Kuramoto model, *Phys. Rev. E* **92**, 022122 (2015).
  - [29] T. Coletta, R. Delabays, and P. Jacquod, Finite-size scaling in the Kuramoto model, *Phys. Rev. E* **95**, 042207 (2017).
  - [30] R. Juhász, J. Kelling, and G. Ódor, Critical dynamics of the Kuramoto model on sparse random networks, *J. Stat. Mech.*, 053403 (2019).
  - [31] K. Harada, Bayesian inference in the scaling analysis of critical phenomena, *Phys. Rev. E* **84**, 056704 (2011).
  - [32] K. Harada, Kernel method for corrections to scaling, *Phys. Rev. E* **92**, 012106 (2015).
  - [33] H. Sakaguchi, Cooperative Phenomena in Coupled Oscillator Systems under External Fields, *Prog. Theo. Phys.* **79**, 39 (1988).